Persistent Sinai-type diffusion in Gaussian random potentials with decaying spatial correlations

Igor Goychuk,[1,*] Vasyl O. Kharchenko,[2] and Ralf Metzler[1]
[1]*Institute of Physics and Astronomy, University of Potsdam, 14476 Potsdam-Golm, Germany*
[2]*Institute of Applied Physics, National Academy of Sciences of Ukraine, 40030 Sumy, Ukraine*
(Received 6 July 2017; published 22 November 2017)

Logarithmic or Sinai-type subdiffusion is usually associated with random force disorder and nonstationary potential fluctuations whose root-mean-squared amplitude grows with distance. We show here that extremely persistent, macroscopic logarithmic diffusion also universally emerges at sufficiently low temperatures in stationary Gaussian random potentials with spatially decaying correlations, known to exist in a broad range of physical systems. Combining results from extensive simulations with a scaling approach we elucidate the physical mechanism of this unusual subdiffusion. In particular, we explain why with growing temperature and/or time a first crossover occurs to standard, power-law subdiffusion, with a time-dependent power-law exponent, and then a second crossover occurs to normal diffusion with a disorder-renormalized diffusion coefficient. Interestingly, the initial, nominally ultraslow diffusion turns out to be much faster than the universal de Gennes–Bässler–Zwanzig limit of the renormalized normal diffusion, which realistically cannot be attained at sufficiently low temperatures and/or for strong disorder. The ultraslow diffusion is also shown to be nonergodic and it displays a local bias phenomenon. Our simple scaling theory not only explains our numerical findings but qualitatively also has a predictive character.

DOI: 10.1103/PhysRevE.96.052134

I. INTRODUCTION

Systems with Gaussian energy disorder characterized by spatially decaying correlations are ubiquitous in physics thanks to the central limit theorem [1,2]. Such systems include, for instance, disordered organic photoconductors with long-range electrostatic interactions [3,4], supercooled liquids [5], as well as naturally occurring DNA macromolecules encoding biological information in living systems [6–8]. Colloidal systems in quenched, random laser-created potentials have also recently become experimentally available [9–12].

A common line of thinking [13] treats diffusion and transport phenomena in such systems as normal on experimentally relevant scales, with a potential disorder-renormalized diffusion coefficient $D_{\rm ren} = D_0 \exp(-[\beta\sigma]^2)$, where D_0 is the free diffusion coefficient of the diffusing particle in absence of the potential, $\sigma = \langle \delta U^2(x)\rangle^{1/2}$ is the root-mean-squared amplitude of the potential fluctuations $\delta U(x)$, and $\beta = 1/(k_B T)$ is the Boltzmann factor proportional to inverse temperature. This famed renormalization result by De Gennes [14], Bässler [5], and Zwanzig [15] corresponds to a common measurable temperature dependence of transport coefficients in disordered glassy systems which is almost indistinguishable from the Vogel-Fulcher-Tammann law [16], another commonly used temperature dependence used to fit experimental data.

It came as a surprise when extensive simulations of stochastic Langevin dynamics in Gaussian random potentials with decaying spatial correlations by Romero and Sancho [17] demonstrated that the emerging diffusion is anomalously slow over the whole time range of simulations and characterized by a power-law scaling $\langle \delta x^2(t)\rangle \propto t^\alpha$ $(0 < \alpha < 1)$ of the mean-squared displacement. This result is very remarkable indeed because within the mean-field approximation it is easy to show that the quenched Gaussian energy disorder yields residence time distributions (RTDs) $\psi(\tau)$ all moments of which are finite [18]. This behavior is fundamentally different from the situation of annealed exponential energetic disorder yielding RTDs of the form $\psi(\tau) \propto 1/\tau^{1+\alpha}$ with $\alpha = k_B T/\sigma$ [19]: Here subdiffusion emerges for $k_B T < \sigma$ because of the divergent mean residence times, which provides the standard model of subdiffusion in the continuous-time random-walk framework [19,20].

Hence, Gaussian energy disorder cannot yield subdiffusion in the absence of spatial correlations. To neglect such correlations is a usual procedure when they are short ranged [13]. Whether organic photoconductors and other disordered materials are better described by Gaussian or exponential models of the energy disorder is a subject of continuing controversy. On the one hand, the Gaussian model is generally accepted for organic photoconductors [3]. On the other hand, some recent experiments [21] seem to be more consistent with the model of exponential disorder, leading to a similar time dependence of transient currents as in amorphous semiconductor films [22]. Models of Gaussian disorder with significant spatial correlations can be a key to resolve this controversy. Physically, for instance, such short-range correlations may correspond to the size of a protein molecule diffusing over the potential landscape of a DNA strand [23] or to the size of a colloidal particle in an uncorrelated laser field potential [10]. Moreover, long-range electrostatic interactions give rise to long-range spatial correlations in organic photoconductors [4], and biological information encoded in the sequence of DNA base pairs manifests itself in long-range base-pair correlations [24,25].

The remarkable discovery that subdiffusion persists beyond the mean-field approximation was reaffirmed in a number of recent studies [11,23,26,27]. It was explained recently in terms of a finite nonergodicity length $L_{\rm erg}$ of the spatial random process $\exp[\beta\delta U(x)]$ [23] related to the presence of spatial potential correlations. In this respect, the origin of a weak ergodicity breaking—the fundamental difference

*Corresponding author: igoychuk@uni-potsdam.de

between ensemble- and time-averaged physical observables even in the limit of long observations times [28–30]—is very different from the one in systems described by continuous-time random walks with annealed, uncorrelated residence time distributions with divergent mean residence times [28,29,31–34]. For systems with Gaussian disorder, the nonergodic behavior occurs on the transient spatial scale $L_{\rm erg}$ which, however, rapidly grows with $\beta\sigma$ for spatially correlated potential fluctuations $\delta U(x)$. Indeed, this spatial scale can readily reach macroscopic sizes already for disorder strengths $\sigma \sim 4$–$5\, k_BT$, which is a typical value for disordered organic photoconductors already at room temperatures [4].

Subdiffusion occurs on the corresponding nonergodic and generally mesoscopic spatial scales. Somewhat surprisingly, diffusion retains its asymptotically normal form for any decaying correlations, no matter how slow they decay [23]. However, for mesoscopic and even macroscopic systems this limit can be out of reach and become physically completely irrelevant, leading us to consider this type of subdiffusion as one of the fundamental processes in a large range of applications. Some of these remarkable features have recently been confirmed experimentally in colloidal systems [11] and, more tentatively, also for diffusion of regulatory proteins on DNA strands [35]. Namely, although in Ref. [35] the results are interpreted in terms of normal diffusion, the single-trajectory diffusion coefficient is scattered over three orders of magnitude, which likely implies a lack of ergodicity. The real physical mechanism of anomalous diffusion in spatially correlated Gaussian energetic disorder remains elusive, and it is the main goal of this paper to clarify its physical origin. The whole setup is very different from the original scenario of Sinai diffusion [1,2,36,37]. It is also different from Sinai diffusion emerging from a power-law energy disorder [25], or logarithmic tails of the waiting time distribution [38] in the mean-field approximation. Notwithstanding, we will show below that a generalized Sinai subdiffusion indeed emerges at sufficiently low temperatures with $\langle \delta x^2(t)\rangle \propto [\ln(t/t_0)]^a$, with a general scaling exponent a, which is $a = 4$ in the special case of Sinai diffusion [1,2,36,37]. The latter one is usually associated with the model of random force disorder [1,2,25,37] yielding potential fluctuations whose root-mean-square amplitude exhibits an unlimited growth with distance, that is, the potential presents a free Brownian motion in space [1,2,37]. A generalized Sinai diffusion with $a \neq 4$ emerges also in the case of fractional Brownian motion in space [39].

In this work, we reveal that a generalized Sinai-type diffusion universally emerges for a sufficiently low temperature and/or strong disorder when $\beta\sigma$ exceeds a typical value of 5 to 10, even for the case of very short-range exponential or linearly decaying correlations. Despite its broad relevance, such logarithmic diffusion has not been revealed and studied in the previous related research including Ref. [23]. This fundamental result is fully confirmed by extensive simulations. Based on the arguments developed herein it should be absolutely possible to observe macroscopic Sinai diffusion at experimentally relevant time scales, in systems governed by spatially correlated Gaussian energetic disorder. Moreover, our theory elegantly describes the transition from Sinai-type diffusion to a standard power-law diffusion with a time-dependent $\alpha(t)$, which can be nearly constant for a sufficiently long time and has a temperature dependence that is reminiscent of annealed exponential disorder, i.e., $\alpha \propto k_BT/\sigma$. Additionally, it predicts that the transition to the normal diffusion regime occurs with a logarithmically growing $\alpha(t) \propto \log(t)$. These predictions clearly beyond [23] and other related work are confirmed with extensive numerical simulations for four different models of spatial correlations decay: exponential, the case of Ref. [23], and also power-law correlations with infinite correlation length, as well as for linearly and Gaussian decaying correlations. Finally, we establish a general type of distribution of the escape times out of a finite spatial domain, which turns out to be a generalized log-normal distribution all moments of which are finite.

The remainder of this manuscript is structured as follows. In Sec, II we develop the general concepts of our approach and introduce a scaling theory for the resulting diffusive dynamics. Section III presents results from extensive simulations for various relevant cases of the spatial correlations decay of the potential fluctuations. In Sec. IV we present a detailed discussion of our results and draw our conclusions.

II. BASIC CONCEPTS AND SCALING THEORY

A. Growing potential fluctuations

We start from an observation, which is central to the theory of extreme events [40] and pivotal for the present study. Namely, even if a stationary Gaussian process $U(x)$ has a finite root-mean-squared fluctuation σ, the maximal amplitude of its fluctuations $\delta U_{\rm max}(x)$ grows slowly with the distance x, at odds with intuition [10,41,42]. The law of this growth can be found from the following treatment. We consider the potential as a random process with zero average, $\langle U(x)\rangle = 0$, and ask the question of how often an energy level $U_{\rm max}$ is crossed with growing distance $x \to \infty$ in a stationary limit. For any stationary, differentiable Gaussian process with normalized autocorrelation function $g(x) = \langle U(x+x')U(x')\rangle/\sigma^2$ and asymptotically decaying correlations, the answer is known: The averaged number of level-crossing events $\langle n(x)\rangle$ grows linearly with distance, $\langle n(x)\rangle = \Gamma x$, at the rate $\Gamma = \sqrt{-g''(0)}\exp(-U_{\rm max}^2/2\sigma^2)/\pi$ [43]. Thus, the level $U_{\rm max}$ is crossed on average at the distance x found from $\langle n(x)\rangle = 1$. Hence, on average,

$$U_{\rm max}(x) = \sigma[2\ln(x/x_0)]^{1/2}, \tag{1}$$

where $x_0 = \pi/\sqrt{-g''(0)}$. This is a very general and universal result valid for any correlations with finite $g''(0)$, known in the mathematical literature, see, e.g., in Ref. [41]. However, it is practically unknown for physicists and our short derivation is new. Note that this result holds only asymptotically, given a stationary regime is established. Moreover, the longer the correlations range, the later this asymptotic result is established.

For example, for a Gaussian decay of the correlations we will have $g(x) = \exp(-x^2/\lambda^2)$ with a correlation length scale parameter λ and in this case $x_0 = \pi\lambda/\sqrt{2}$. Note that in a scaling sense such a correlation length parameter λ always exists, even if the correlation length formally defined as $\lambda_{\rm corr} = \int_0^\infty |g(x)|dx$ may diverge. The length λ plays a fundamental role in the presence of correlations. It can be, for instance, of

the size of the protein–DNA contact or the size of the colloidal particle in an uncorrelated laser field.

For power-law decaying correlations with $g(x) = 1/[1 + x^2/\lambda^2]^{\gamma/2}$, and $g(x) \propto 1/x^{\gamma}$ for $x \gg \lambda$, and thus $x_0 = \pi\lambda/\sqrt{\gamma}$. This case is very interesting in applications to diffusion of regulatory proteins on DNA strands, where the real base-pair sequence arrangement can play a very profound role [44,45]. In particular, long-range correlations in the base-pair sequence, which encode biological information, can indeed decay algebraically slow, as shown, for instance, in Refs. [24,25] with $\gamma \sim 0.6$–0.8. This should yield corresponding correlations in the protein binding energy with λ being of the size of the protein–DNA contact or larger. Namely, we here have a case for which $\lambda_{\rm corr} \to \infty$, which suggests that the subdiffusive regime should hold much longer than in the case of short-ranged correlations. This is indeed confirmed in our detailed analysis below. Another important example is provided by some organic photoconductors, for which $\gamma = 1$ and $\sigma = 0.1$–0.125 eV or 4–5 k_BT at room temperature [4].

The next case of relevance we consider here is the Ornstein-Uhlenbeck process with $g(x) = \exp(-|x|/\lambda)$. This case may at first appear problematic as it is not differentiable, and the corresponding force $f(x) = -\partial V(x)/\partial x$ has the infinite root-mean-squared amplitude $\langle f^2(x)\rangle^{1/2} \to \infty$. However, in physical applications we consider in fact a regularized Ornstein–Uhlenbeck process on a lattice with a finite grid size Δx. This allows also for a numerical treatment of the corresponding continuous dynamics (which otherwise would not be possible due to the infinite force root-mean-squared amplitude). We note that this point is similar to the subtleties arising when we consider the model of white Gaussian processes $f(x)$ in the theory of continuous space Sinai diffusion [1]. Indeed, we always generate realizations of Gaussian processes with some finite resolution Δx, following a well established algorithm [46]. The corresponding $g(x)$ becomes, in fact, thereby regularized. An appropriate formal regularization reads $g(x) = \exp[-\sqrt{x^2 + (\Delta x/2)^2}/\lambda + \Delta x/(2\lambda)]$. It yields the same force root-mean-squared $\langle f^2(0)\rangle^{1/2} = \sqrt{2}\sigma/\sqrt{\Delta x\lambda}$ as the Ornstein–Uhlenbeck process on a lattice with grid size Δx. In this case, $x_0 = \pi(\lambda\Delta x/2)^{1/2}$. An important further remark is that, when $\Delta x \to 0$, then $x_0 \to 0$, and $U_{\rm max}(x)$ grows accordingly for any fixed x. However, this growth is logarithmically slow, and for realistic variations of Δx the effect is small. Nevertheless, the case of exponentially decaying correlations is especially interesting in the present context. Notice that such short-range correlations appear also in the case of a biologically meaningless and completely random DNA because of a finite size λ of the protein–DNA contact, which is typically from 5 to 30 base pairs [47].

It should also be mentioned that the shortest possible correlation range corresponds to the case when the values of the potential are completely independent on all the lattice sites. This does not mean, however, that $U(x)$ is delta correlated because $U(x)$ is continuous, which introduces correlations within a $\pm\Delta x$ neighborhood of any lattice site. In such a situation, $\langle U(x' + x)U(x')\rangle$ depends actually on x' within the correlation range. Hence, the corresponding continuous energy disorder is not stationary, which implies that the de Gennes–Bässler–Zwanzig result is not valid asymptotically.

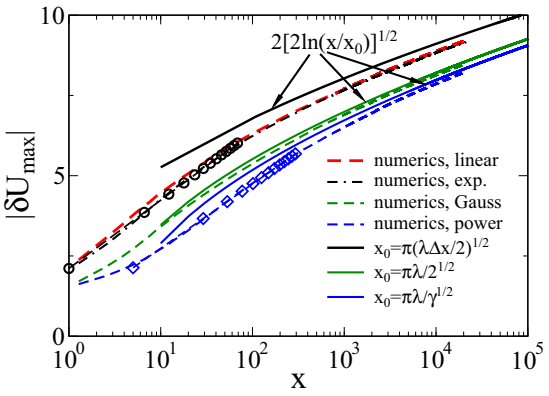

FIG. 1. Maximal amplitude of potential fluctuations $|\delta U_{\rm max}(x)|$ (in units of the root-mean-squared amplitude of fluctuations σ) starting from some random point regarded as the origin, plotted versus distance x (in units of the correlation length λ) for several models of Gaussian potentials with decaying correlations. This decay is (i) exponential, (ii) linear, (iii) Gaussian, and (iv) of power-law form with $\gamma = 0.8$. Broken lines represent the results from simulations and full lines depict the corresponding theoretical results for $|\delta U_{\rm max}| = 2U_{\rm max}(x)$ from Eq. (1), which are gradually approached for long distances x. In all cases, $\Delta x = 0.02$ is chosen. The symbols show a log x scaling fit for either initial or intermediate values of x in the case of exponential and power-law models of the correlations, respectively. Averaging over 10^3 different starting points in 10^2 different potential realizations is done in each case.

Strikingly enough, in this case Eq. (1) also works with $x_0 = \Delta x$, as it can be deduced from the results on uncorrelated Gaussian variables in the classical work on the extreme value distributions by Fisher and Tippett [48]. Notice that in this limiting case the fluctuations of $U_{\rm max}$ are actually larger than in all the models considered in this work, which implies that diffusion can also be transiently anomalously slow for a strong disorder $\beta\sigma \gg 1$. This is indeed so, and, moreover, anomalous diffusion is even slower in absolute terms than the one considered in this paper. This *a priori* surprising special case requires a separate detailed study, which is beyond the scope of this work.

Another pertinent correlation model for the particular application of diffusion on DNA is the model of linearly decaying correlations $g(x) = (1 - |x|/\lambda)$ for $|x| \leqslant \lambda$ and zero otherwise [49]. It emerges when the protein interacts locally with only one corresponding base pair, in the immediate contact. The corresponding random process $U(x)$ is also nondifferentiable, and with respect to the $U_{\rm max}(x)$ behavior its regularized version behaves rather similar to that of the Ornstein–Uhlenbeck process (considered with the same Δx).

Let us check the above exact analytical results against the results from extensive simulations: Figure 1 shows how the amplitude of the potential fluctuations $|\delta U_{\rm max}| = U_{\rm max}(x) - U_{\rm min}(x) = 2U_{\rm max}(x)$ grows with distance for several models of Gaussian disorder. The universal result in Eq. (1) agrees well with the numerics for all four models considered here. A similar scaling was also found numerically for a different model of correlations [10]. The agreement is better for differentiable (in the limit $\Delta x \to 0$) processes, and the model of linearly decaying correlations behaves indeed rather

similarly to the Ornstein–Uhlenbeck model. Notice that in the case of power-law decaying correlations with $\gamma = 0.8$, the convergency is slower than for the Gaussian decay, and for much smaller γ, for instance, $\gamma = 0.2$, it is still far from being achieved for the largest x in Fig. 1 (not shown). The results in Fig. 1 are obtained from a well-known spectral method [46] given the corresponding correlation functions on a lattice with grid size Δx ($\Delta x = 0.02$ in Fig. 1) and a maximal spatial interval $L_{\max}$ ($L_{\max} = N\Delta x, N = 2^{20}$ in Fig. 1). Notice also that the exact behavior of the function $g(x)$ is used to generate the realizations of the Ornstein–Uhlenbeck process and the process with linearly decaying correlations. The shown results are obtained from averaging over 10^3 uniformly distributed points (particles) in each potential realization, and 10^2 such potential realizations for each model of correlations were taken.

It is clear that the strongest potential fluctuations occur in the case of exponential and linear correlations. They are further increasing for smaller values of the resolution Δx due to the singularity of these models. Another salient feature is that another scaling can be observed transiently. Namely, we initially find the behavior $\log x$ rather than the $\sqrt{\log x}$ scaling for the exponential and linear correlations and intermediately for the case of power-law decaying correlations. Moreover, we notice an initial $(\log x)^{\delta}$ scaling with $\delta > 1$ for the power-law and Gaussian decay. To account for these various behaviors we henceforth consider the following model:

$$|\delta U_{\max}(x)| = \sigma_{\text{eff}}[\ln(x/x_{\text{in}})]^{\delta} \tag{2}$$

for the potential fluctuations, where σ_{eff}, δ, and x_{in} are fitting parameters, which are generally different from the theoretical values $\sigma_{\text{eff}} = 2\sqrt{2}\sigma \approx 2.83\,\sigma, \delta = 1/2$, and $x_{\text{in}} = x_0$ in Fig. 1. Notice that δ is not a free fitting parameter but rather a function of distance and, hence, of time in diffusion dynamics, with the asymptotic value $1/2$. It will be fixed below to either 1 or $1/2$, which provides both a sufficient accuracy and important insights. We will now use this generic empirical formula and pursue the scaling argumentation used originally in the case of continuous space Sinai diffusion [1].

B. Scaling theory

Let us estimate the time t a particle needs to travel the distance x starting at x_0, limited in an Arrhenius manner by the largest barrier met on its way, $t = t_0 \exp[\beta|\delta U_{\max}(x)|]$, where t_0 is a proportionality factor of physical unit of time. From this scaling ansatz, in combination with relation (2), we immediately obtain our central result for the mean-squared displacement of the diffusing particle,

$$\langle \delta x^2(t)\rangle = x_{\text{in}}^2\{e^{[(k_BT/\sigma_{\text{eff}})\ln(t/t_0)]^{1/\delta}} - 1\}^2. \tag{3}$$

This in turn yields the asymptotic form

$$\langle \delta x^2(t)\rangle \approx x_{\text{in}}^2[(k_BT/\sigma_{\text{eff}})\ln(t/t_0)]^{2/\delta} \tag{4}$$

for small temperatures and/or strong disorder, $k_BT/\sigma_{\text{eff}} \ll 1$. For $\delta = 1/2$, this is precisely the Sinai-type diffusion with $a = 2/\delta = 4$. Notice, however, that such a logarithmic scaling in time is derived typically from the scaling $\delta U_{\max}(x) \propto \sqrt{x}$ of nonstationary potential fluctuations with distance [1]. This corresponds to a Brownian motion of the potential in space. In our case, the physical origin of this diffusion is very different. It corresponds to a transient regime, which can, however, be extremely persistent, see below. Furthermore, for $\delta = 1$, $\langle \delta x^2(t)\rangle \approx x_{\text{in}}^2[(k_BT/\sigma_{\text{eff}})\ln(t/t_0)]^2$. Generally, we can consider $a = 2/\delta$ as a fitting parameter for generalized Sinai diffusion in Eq. (4). However, it is not considered a free fitting parameter in Eq. (3).

Next, with increasing temperature and time, when the unity becomes negligible in Eq. (3), we find the intermediate behavior

$$\langle \delta x^2(t)\rangle \approx x_{\text{in}}^2[t/t_0]^{\alpha(t)} \tag{5}$$

with the time-dependent scaling exponent

$$\alpha(t) = 2(k_BT/\sigma_{\text{eff}})^{1/\delta}\ln^{1/\delta-1}(t/t_0). \tag{6}$$

This result predicts a power-law subdiffusion with a gradually changing anomalous diffusion exponent. It should be mentioned here that this result follows from the approximation $\exp[f(t)] - 1 \approx \exp[f(t)]$, for a logarithmically growing $f(t)$, which is not fully accurate in our numerics. Nevertheless, it predicts the correct law for $\alpha(t)$, namely, $\alpha(t) \propto \log t$, for $\delta = 1/2$, see below. This result is especially insightful for $\delta = 1$ (or $\log x$ scaling): Here $\alpha(t) = 2k_BT/\sigma_{\text{eff}} = \alpha_{\min}$, and we observe subdiffusion of power-law form with a constant anomalous diffusion exponent. Moreover, given the results depicted in Fig. 1, where initially $\delta > 1$, intermediately $\delta = 1$, and asymptotically $\delta = 1/2$, one can predict that initially $\alpha(t)$ will diminish and reach a minimum and then logarithmically increase in time. This is what we actually see in the simulations with $\sigma_{\text{eff}} \approx (1.24\text{–}1.52)\sigma$ within the temperature range $\sigma/4 < k_BT < \sigma/2$, see below. Such a behavior may indeed mistakingly be attributed to continuous-time random-walk subdiffusion.

C. Normal diffusion limit

Due to the decaying correlations of the Gaussian potential fluctuations in our model, with increasing temperature for a given root-mean-squared amplitude σ (decreasing $\beta\sigma$) and for times longer than a certain crossover time, a transition to normal diffusion will gradually emerge. The normal diffusion coefficient can be derived from the Lifson–Jackson expression [13,50]

$$D_{\text{ren}} = \frac{D_0}{\overline{C_L^+}\,\overline{C_L^-}} \tag{7}$$

for the diffusion coefficient in periodic potentials with spatial period $L_{\max}$, where $\overline{C_L^{\pm}} = \frac{1}{L_{\max}}\int_0^{L_{\max}} e^{\pm\beta U(x)}dx$ is a spatially averaged statistical weight function $w_{\pm}(x) := e^{\pm\beta U(x)}$ and D_0 is the free space diffusion coefficient. This averaging [15] involves a very large $L_{\max} \to \infty$ and replacing the spatial average with the ensemble average, i.e., $\overline{C_L^{\pm}} \to \langle w_{\pm}(x)\rangle$, which is $\langle w_{\pm}(x)\rangle = e^{(\beta\sigma)^2/2}$ for an unbiased Gaussian $U(x)$. Clearly, $w_{\pm}(x)$ must be ergodic for this substitution, just per definition, and ergodicity requires, first, stationarity of the random process $U(x)$ under consideration [43].

TABLE I. Nonergodicity length $L_{\rm erg}$ from Eq. (8), in units of λ and values for $e^{\beta^2\sigma^2}$.

$g(x)$	$\beta\sigma = 2$	$\beta\sigma = 3$	$\beta\sigma = 4$	$\beta\sigma = 5$	$\beta\sigma = 10$
$e^{-\lvert x\rvert}$	34.85	2070	1.2×10^6		
e^{-x^2}	51.89	5027			
$\frac{1}{(1+x^2)^{\gamma/2}}$, $\gamma = 0.8$	166.83	9670	6.86×10^6	4.28×10^{10}	7.64×10^{42}
$1 - \lvert x\rvert$	24.59	1798	1.11×10^6	5.76×10^9	5.37×10^{41}
$e^{\beta^2\sigma^2}$	54.59	8103	8.89×10^6	7.20×10^{10}	2.69×10^{43}

D. Transient lack of ergodicity

However, even for a stationary and ergodic $U(x)$ there exists a characteristic length $L_{\rm erg}$ on which fluctuations of $w_\pm(x)$ do not self-average out. This transient lack of self-averaging in space is accompanied by anomalous diffusion of nonergodic nature in time on the corresponding spatial scale. The point is that the particles explore on this scale $L_{\rm erg}$ locally very different realizations of the potential landscape, with a large variation of the statistical weight function $w_\pm(x)$ containing, in fact, the probability of thermally activated jumps over local barriers. The corresponding diffusion process is clearly nonstationary in increments, and this leads to a transient lack of ergodicity and aging phenomena [30,51]. Already Eq. (7) suggests that the local $D_{\rm ren}$ should be very different in this case and strongly scattered. Then, however, actually diffusion in this case cannot be characterized by a normal diffusion coefficient, as it becomes anomalous. This typical length can be found from the condition that the variance of the random process $w_\pm(x)$ equals the mean, which yields the following implicit equation for this, so far unknown, characteristic length $L_{\rm erg}$ [23],

$$\int_0^1 (1-y)e^{\beta^2\sigma^2 g(L_{\rm erg}y)}dy = 1. \tag{8}$$

This equation was derived under the assumption [23] that $U(x)$ is a stationary process. The transition to normal diffusion starts at $\langle \delta x(t)^2\rangle \gtrapprox L_{\rm erg}^2$. However, this transition may last extremely long, and anomalous diffusion features may persist for appreciably long times for $|\delta x| > L_{\rm erg}$.

For the case of linearly decaying correlations, Eq. (8) can be solved exactly, and we obtain ($L_{\rm erg} > \lambda$)

$$L_{\rm erg} = \frac{\lambda}{(\beta\sigma)^2}\{(e^{\beta^2\sigma^2} - 1) - (\beta\sigma)^2 + [2(\beta\sigma)^4 + 4(\beta\sigma)^2 - 2(\beta\sigma)^2 e^{(\beta\sigma)^2} + 3 - 4e^{(\beta\sigma)^2} + e^{2(\beta\sigma)^2}]^{1/2}\}, \tag{9}$$

which for $\beta\sigma \gtrapprox 2.5$ is approximated by the simple expression

$$L_{\rm erg} \approx \frac{2\lambda}{(\beta\sigma)^2}e^{(\beta\sigma)^2} \tag{10}$$

with a very good accuracy. For other models of $g(x)$, Eq. (8) is solved numerically, the results being listed in Table I for several values of $\beta\sigma$. One can see that the shortest length $L_{\rm erg}$ occurs for the linearly decaying correlations and the longest one for the power-law correlations. Somewhat surprisingly, for the Gaussian decay the nonergodicity length is larger than for exponentially decaying correlations.

One can also use Eq. (10) with Δx instead of λ to roughly estimate the nonergodicity length in the case of potential values which are uncorrelated on the distance of a lattice constant, with correlations decaying to zero within $\pm\Delta x$ of any lattice site. Of course, this estimate cannot be rigorous because Eq. (8) is, strictly speaking, not valid for a nonstationary $U(x)$ featuring this problem. Nevertheless, it suggests that $L_{\rm erg}$ can also be very large in this case for $\beta\sigma \gg 1$. This case is left for a separate study.

As mentioned above, there exist several crossover times in the dynamics. The first one corresponds to the transition from Sinai like diffusion to the power-law diffusion regime. The corresponding transition time τ^* can be roughly estimated from the condition that the argument of the exponential function in Eq. (3) reaches unity. From this, $\tau^* \sim t_0 \exp[\sigma_{\rm eff}/k_BT]$. It grows exponentially fast with $\sigma_{\rm eff}/k_BT$. The second transition time $\tau_{\rm erg}$ can be estimated from the condition of how long the power-law diffusion regime with anomalous diffusion exponent $\alpha_{\rm min} \approx 2k_BT/\sigma_{\rm eff}$ will last. Thus we find the conditions $\langle x^2(t)\rangle \sim x_{\rm in}^2(\tau_{\rm erg}/t_0)^{\alpha_{\rm min}} \sim L_{\rm erg}^2$, from which with $\alpha_{\rm min} \approx 2k_BT/\sigma_{\rm eff}$ and Eq. (10), we obtain the estimate

$$\tau_{\rm erg} \sim t_0\left[\frac{4\lambda^2}{x_{\rm in}^2}\frac{(k_BT)^4}{\sigma^4}\right]^{\frac{\sigma_{\rm eff}}{2k_BT}} \exp\left[\frac{\sigma^2\sigma_{\rm eff}}{(k_BT)^3}\right]. \tag{11}$$

Notice the superexponential growth of $\tau_{\rm erg}$ with $\sigma/(k_BT)$. This is precisely the reason why the power-law subdiffusion regime can last so long for even moderate values $\sigma/(k_BT) \sim 4$–5, and no transition to the regime of normal diffusion was revealed in the concrete cases studied in Refs. [17,26,27].

III. RESULTS OF NUMERICAL SIMULATIONS

We now proceed by checking our theoretical predictions against results of extensive numerical simulations, finding remarkable agreement. To this end, let us consider a continuous-space Brownian dynamics governed by the overdamped Langevin equation

$$\eta\frac{dx(t)}{dt} = -\frac{dU(x)}{dx} + \sqrt{2k_BT\eta}\times\zeta(t), \tag{12}$$

where η is the frictional coefficient and $\zeta(t)$ is unbiased, white Gaussian noise with δ correlation $\langle\zeta(t)\zeta(t')\rangle = \delta(t-t')$. Distance is scaled in units of λ, time in units of $\tau_0 = \lambda^2\eta/\sigma$, and temperature in σ/k_B. Initially, 10^4 particles are uniformly distributed in random potentials (10 realizations), and the particle motion is integrated using periodic boundary conditions with a very large period $L_{\rm max}$. The random potential is generated on a lattice with spacing $\Delta x = 0.02$, and discrete points are connected by parabolic splines, that is, the potential is locally parabolic, and the corresponding force entering the Langevin equation (12) is piecewise linear. In this respect our

setup is similar to the one considered in Refs. [17,23,27], but different from that in Refs. [10,11], where a discrete hopping dynamics in both space and time was studied. In most simulations, we employ $L_{\max} = 2^{19}\Delta x \approx 1.0485 \times 10^4 \lambda$. We use the stochastic Heun method with a time integration step $\Delta t = 2 \times 10^{-4}$ in most simulations. For disorder which is uncorrelated on the lattice sites, $\Delta t = 2 \times 10^{-5}$.

A. Ensemble-averaged diffusion

We start our numerical analysis with the case of ensemble-averaged diffusion. From the simulated trajectories, we perform an ensemble averaging to obtain the mean-squared displacement.

1. Exponential correlations

Let us focus first on the case of the exponentially decaying correlations, $g(x) = \exp(-|x|)$. The results are depicted in Figs. 2(a) and 2(b). In Fig. 2(a), the fit of the numerical results is based on Eq. (3) using $\delta = 1/2$, $\sigma_{\text{eff}} \sim 4$–$4.7$, and $x_{\text{in}} \sim 0.59$–5.01. Note that the fitting values σ_{eff} differ only by a factor of less than two from the theoretical value 2.83 in Fig. 1. The difference emerges because many barriers are present on the diffusion pathway and in the scaling theory we approximate this complex picture by introducing just a single effective barrier on the pathway with a height which corresponds to the maximal amplitude of the fluctuations, i.e., the difference between the maximal and minimal values of the potential energy landscape met on this pathway. Hence, a "less than factor two" discrepancy is, in fact, reassuring. The corresponding theoretical value x_0 is $x_0 \approx 0.31$. Here, the agreement is worse, however, the numerical results in Fig. 1 in this case are also somewhat different from the theoretical asymptotics, which are still not reached. The same numerical data are fitted by expression (3) with $\delta = 1$ in Fig. 2(b), with $\sigma_{\text{eff}} \sim 1.23$–$1.69$. For $T = 0.1$ and $T = 0.2$, both fits have almost the same quality, although the fit with $\delta = 1$ appears slightly better. For $T = 0.1$, Sinai-like diffusion (4) with $a \approx 3.7$, near to the Sinai value $a = 4$, covers about 6 decades in time, Fig. 2(b). It is worth noting that for $T \leqslant 0.25$ the fit with $\delta = 1$ works better, see Fig. 2(b), due to the initial $\log x$ scaling in Fig. 1 (see symbols therein). For this reason, $\alpha(t)$ shows a nearly constant behavior, at intermediate temperatures, for an extended time period, Fig. 3(a). In fact, in this regime the power-law exponent is nearly proportional to temperature, $\alpha \approx 2k_BT/\sigma_{\text{eff}}$, where the value of σ_{eff} is obtained from fitting the minimal value $\alpha_{\min}$ in Fig. 3(a) by this dependence. It turns out that $\sigma_{\text{eff}} \approx 1.52$, Fig. 4. However, with increasing temperature, when diffusion covers larger distances, the fit with $\delta = 1/2$ becomes much better [compare the case $T = 0.5$ in Figs. 2(a) and 2(b)]. An excellent fit holds over about 6 to 7 decades in time with $\delta = 1/2$, where the explicit time dependence of the anomalous diffusion exponent $\alpha(t)$ in Eq. (5) becomes apparent for sufficiently long times. Notice that at the end point of the simulations in Fig. 2(a) for $T = 0.5$ the transition to the renormalized normal diffusion regime is almost accomplished. Strikingly enough, Eq. (3) describes the behavior nicely almost over the entire range of simulations. At larger temperatures, for instance, $T = 1$, the crossover to the asymptotic regime of normal diffusion is already completely accomplished up to $t_{\max} = 10^6$ in our simulations. Such high temperatures, or weak disorder strengths, are not of interest for anomalous diffusion of the kind discussed. Generally, α_{eff} reaches a minimum $\alpha_{\min}$, may stay nearly constant for a certain time period, and then logarithmically increases, a dependence which can be fitted by Eq. (6) with $\delta = 1/2$ and some values of σ_{eff} and t_0, which are different from those used in Fig. 2(a), see Fig. 3(a) for $T = 0.5$ and $T = 1/3$. The reason for this discrepancy in the corresponding fitting values is that a transition from Eq. (3) to Eqs. (5) and (6) is still not quite justified numerically. Nevertheless, the prediction of a logarithmically increasing $\alpha(t)$, as confirmed by the simulations, is a remarkable success of our simple scaling theory.

Interestingly, our simulations demonstrate that, generally, the observed subdiffusion is much faster than the corresponding limit of disorder-renormalized normal diffusion, which is also shown in Fig. 2(a) for several values of the temperature. The presence of correlations thus leads to a dramatic increase in the particle mobility on intermediate but relevant time scales. Note that, whereas for $T = 0.5$ this limit is already gradually approached in Fig. 2(a), the corresponding asymptotics cannot even be depicted for $T = 0.2$ and $T = 0.1$ in this figure, as they lie outside of the plotting range and, therefore, are completely irrelevant on the corresponding time scale.

2. Power-law correlations

We proceed with the case of power-law correlations of the spatial potential fluctuations, with $\gamma = 0.8$. The ensemble averages for the mean-squared displacement are depicted in Fig. 2(c). Here the fit with $\delta = 1$ works generally better, which can be rationalized from Fig. 1, and for $T = 0.1$ a generalized Sinai diffusion with $a \approx 3$ nicely fits the numerical data over 6 decades in time. Note in Fig. 3(b) that $\alpha(t)$ stays nearly constant over 5 decades in time, up to the end of the simulations even for $T = 1/3$. For the larger $T = 0.5$, it also grows logarithmically in time, as in the case of exponential correlations. Why $\alpha(t)$ changes slower in time in this case and a fit with $\delta = 1$ and $\sigma_{\text{eff}} \approx 1.41$ works nicely over many time decades for intermediate temperatures can be rationalized from the fact that the nonergodicity length L_{erg} in this case is much larger, see Table I. The case of power-law correlations is especially important for the diffusion of regulatory proteins on DNA strands, where such long-range correlations with $\gamma \sim 0.6$–0.8 emerge due to the way biological information is encoded in the base-pair sequence. Our results imply that such diffusion should be typically anomalously slow with $\alpha \sim 1.41\ k_BT/\sigma$ in the corresponding range of temperatures for $\gamma = 0.8$. It must be stressed in this respect that diffusion does not become immediately normal for $\langle \delta x^2(t) \rangle > L_{\text{erg}}^2$, but rather a very slow crossover with growing $\alpha(t)$ emerges, see Fig. 2(c) for $T = 0.5$. Here, the transition to the asymptotic regime of normal diffusion is still far from being established.

Somewhat surprisingly, for power-law correlations subdiffusion is essentially faster in absolute terms than in the case of exponentially short correlations, see Fig. 5. This may at first appear counterintuitive. However, one reason for this feature becomes clear from the potential fluctuations

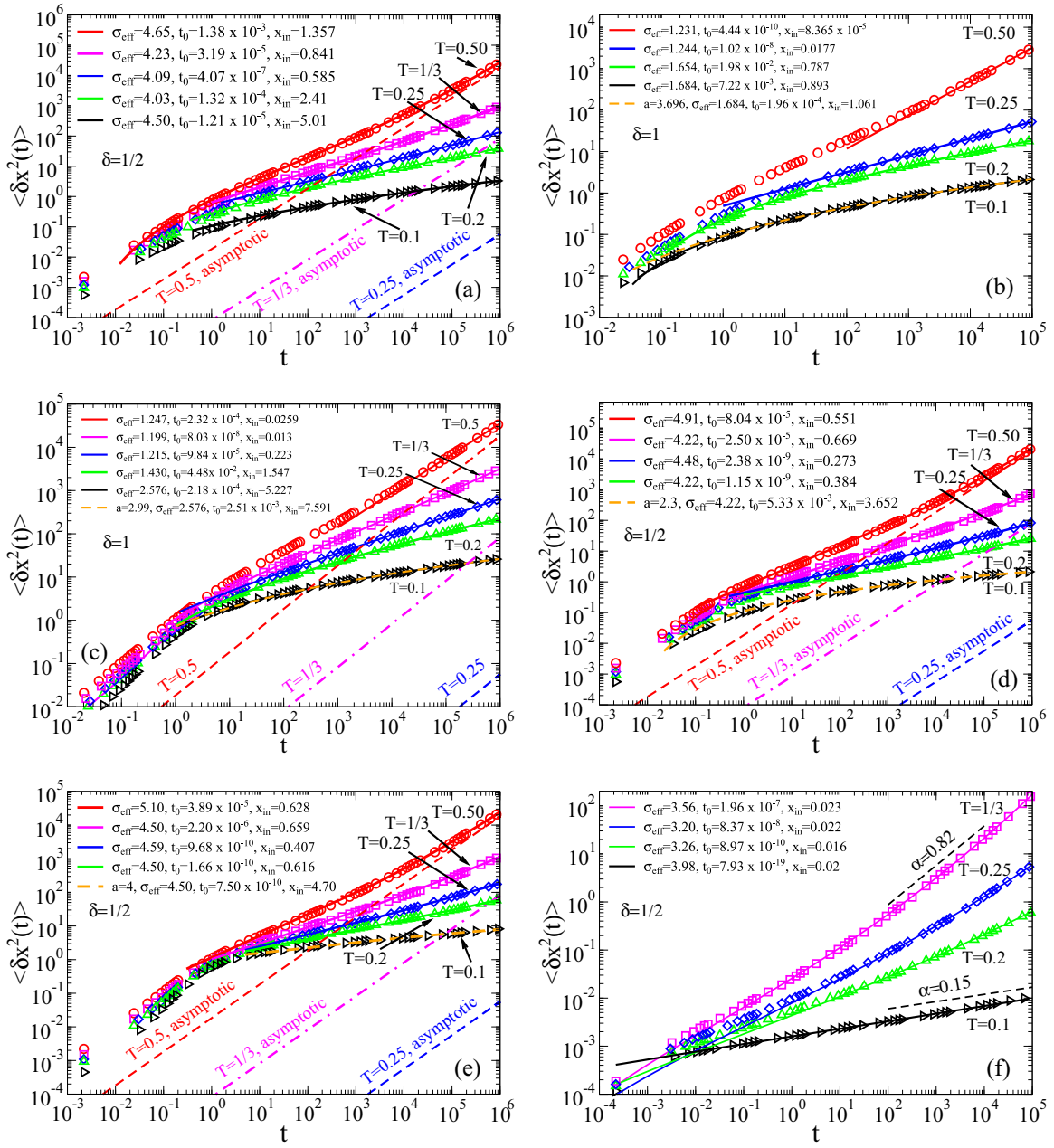

FIG. 2. Ensemble-averaged mean-squared displacement (symbols) for different values of k_BT in units of the disorder strength σ for the four different models of spatial correlation decay: [(a) and (b)] exponential decay, (c) power-law decay with $\gamma = 0.8$, (d) linear decay, (e) Gaussian decay, and (f) potential which is uncorrelated on lattice sites and piecewise linear in between. The fit of the numerical results (full lines) is performed with expression (3) using $\delta = 1/2$ in (a), (d), (e), and (f) and $\delta = 1$ in (b) and (c). The dashed orange line in (b) to (d) shows an alternative fit with the generalized Sinai diffusion expression (4) and $a \approx 3.70$ in (b), $a \approx 2.99$ in (c), $a \approx 2.3$ in (d), and $a \approx 4$ in (e). For $T = 0.1$, Sinai diffusion covers typically at least 6 decades of time. Even for $T = 0.5$ the fit with Eq. (3) and $\delta = 1/2$ turns out to be very good over 6 decades of time, as seen in panels (a), (d), and (c). For $\delta = 1/2$, σ_{eff} is typically in the range, $\sigma_{\text{eff}} \sim 4$–$5.1$, whereas for $\delta = 1$ it typically ranges within $\sigma_{\text{eff}} \sim 1.2$–$1.7$. Distances are measured in units of λ and time in units of $\tau_0 = \lambda^2\eta/\sigma$, with the lattice constant $\Delta x = 0.02$.

depicted in Fig. 1, which for the exponential correlations are essentially larger (thinking in units of k_BT). Clearly, exponential correlations and other singular (in the limit $\Delta x \to 0$) models of static disorder present a preferred case to observe Sinai-type diffusion in such systems. The second explanation is that in the case of power-law correlations a local bias is present on a much longer scale. This leads to an essential acceleration of diffusion in the ensemble sense, see Fig. 6(b), where the ensemble mean-squared displacement is in fact superdiffusive [see also Fig. 3(b) for the initial regime] within several scaling lengths at $T = 0.2$. Remarkably, it is even faster than the potential free diffusion. This is namely due to the presence of a local bias, which is also the reason for the Golosov phenomenon in Sinai diffusion, see below.

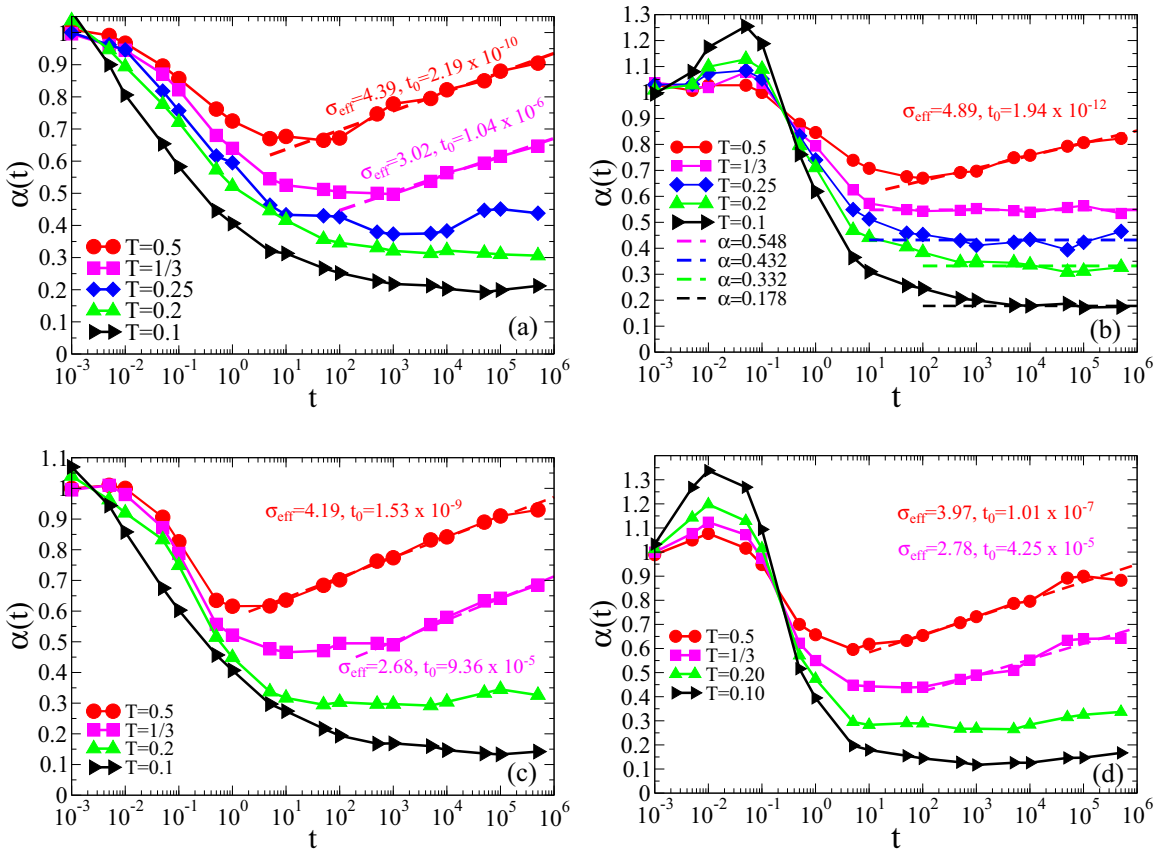

FIG. 3. Time-dependent power-law exponent $\alpha_{\rm eff}(t)$ for an assumed subdiffusive law $\langle \delta x^2(t)\rangle \simeq t^{\alpha(t)}$ obtained as the logarithmic derivative of the traces in Fig. 2, for different temperatures in the case of (a) exponential correlations, (b) power-law correlations with $\gamma = 0.8$, (c) linearly decaying correlations, and (d) Gaussian correlation decay. Symbols connected by lines correspond to numerical results, while the dashed lines are fits to the dependence $\alpha(t) = 2(k_B T/\sigma_{\rm eff})^2 \ln(t/t_0)$. Fitting parameters shown in the plot.

3. *Linear correlations*

The case of linear correlations presents another important model of singular disorder with potential fluctuations growing with diminishing Δx. Therefore, it is expected to be similar to the case of exponential correlations, despite the fundamental difference between these two models. The nonergodicity length $L_{\rm erg}$ here is the shortest within the four considered models, see Table I. The ensemble-averaged mean-squared displacement is depicted in Fig. 2(d). Qualitatively, it appears very similar to the previous cases, however, it turns out to be the slowest one, as Fig. 5 reveals. In this case, $\sigma_{\rm eff} \sim 4.22$–$4.91$, and $x_{\rm in} \sim 0.27$–0.67, except from $T = 0.1$, where $x_{\rm in} \approx 3.65$. Now, the agreement with $x_0 \approx 0.314$ is much better. It might seem paradoxical that the shortest correlations, which exactly vanish at distances exceeding λ, yield the slowest diffusion. However, it must be kept in mind that in the absence of spatial correlations we should have just normal diffusion, which is orders of magnitude slower than the considered correlation-induced subdiffusion. We mention once more that the case of fully uncorrelated disorder simply cannot be realized physically in the case of continuous diffusion with a bounded potential root-mean-square amplitude: The minimal correlation length is $2\Delta x$. The time behavior of the anomalous diffusion exponent $\alpha(t)$ is indeed more similar to the one in the case of exponential correlations than to the case of power-law correlations, see Fig. 3(c), and compare with Figs. 3(a) and 3(b). Notice that the scaling theory nicely describes the transition from the anomalous to the normal diffusion regime over 7 time decades for $T = 0.5$, see Fig. 2(d), where the normal diffusion regime is almost achieved at the end point of simulation.

4. *Gaussian correlations*

Furthermore, we consider the case of Gaussian spatial correlations. Judging from Fig. 1, it should be the second fastest of the four models considered here. This is indeed the case, as seen in Fig. 5. The ensemble-averaged mean-squared displacements display very similar generic features as in the other cases, see Fig. 2(e). Here, $\sigma_{\rm eff} \sim 4.50$–$5.10$ and $x_{\rm in} \sim 0.41$–4.70, whereas the theoretical is $x_0 \approx 2.22$. Once again, the discrepancy by a factor of less than two with the theoretical $\sigma_{\rm eff} = 2.83$ and at least the correct order of magnitude for $x_{\rm in}$ are quite impressive, given the simplicity of our scaling argumentation. Sinai-type diffusion with $a = 4$ is featured in the low temperature behavior at $T = 0.1$. In this case, however, $\alpha(t)$ already starts to slightly increase at the end of the simulations already at $T = 0.1$, Fig. 3(d). This type of correlations indeed presents the worst case to observe a Sinai-like diffusion. The reasons are quite obvious: Namely,

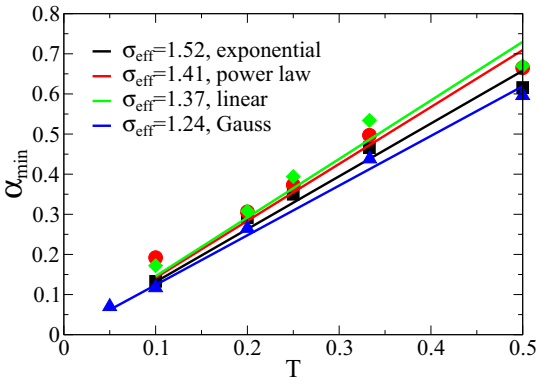

FIG. 4. Dependence of $\alpha_{\min}$ on temperature T for the four different models of spatial correlations discussed in this paper, and the corresponding best linear fits with the dependence $\alpha \approx 2k_BT/\sigma_{\rm eff}$. The values of the corresponding $\sigma_{\rm eff}$ are shown in the plot.

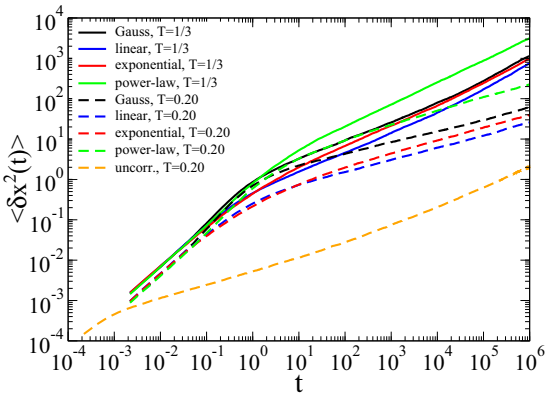

FIG. 5. Comparison of the ensemble-averaged mean-squared displacement for the four different models of the correlation decay and for two values of temperature. Seemingly counterintuitively, the mean-squared displacement is the largest in the case of power-law spatial correlations, where the spatial nonergodicity scale is the longest. Moreover, diffusion is slowest in the case of linear correlations, where the nonergodicity length is the shortest in all four cases, see Table I. In the case of disorder which is uncorrelated on the lattice sites, subdiffusion is even slower in absolute terms, see the lowest orange curve for $T = 0.2$. This special case is, however, not studied in detail in this work.

(1) this model of disorder is not singular and (2) the correlations are short ranged.

5. *Disorder which is uncorrelated on sites*

Finally, for disorder which is uncorrelated on sites, the scaling theory works also remarkably well, as can be deduced from Fig. 2(f). Therein we present the numerical results obtained within the model of a piecewise linear potential (piecewise constant quenched Gaussian force, which is anticorrelated on neighboring sites). Defying intuition, in this scenario diffusion is also transiently anomalously slow. This is because *continuous* potential fluctuations are in fact strongly correlated over nearly two lattice constants. This anomalous diffusion regime can cover many decades of time. The detailed study of this *a priori* paradoxical case is left for a separate investigation. We only comment that in this case the resulting subdiffusion is the slowest one, in absolute terms, as it can be deduced from Fig. 5 for $T = 0.2$. This is because random potential fluctuations are the largest in Eq. (1) with $x_0 = \Delta x$.

B. Single-trajectory averages

As discussed above, the physical origin of the observed subdiffusion is due to a weak breaking of ergodicity. Hence, single trajectory time averages

$$\overline{\delta x^2(t)}^{T_w} = \frac{1}{T_w - t}\int_0^{T_w - t} [\delta x(t|t')]^2 dt' \qquad (13)$$

of the mean-squared displacement $\delta x(t|t') = x(t + t') - x(t')$ over the time window T_w are expected to be very different from the above ensemble result, and their amplitudes should be broadly scattered [30,33]. This is indeed so, as evidenced for all considered models of correlations in Fig. 6, where at all times $t \ll T_w$, and hence this scatter is not a trivial statistical effect occurring when $t \sim T_w$. Remarkably, some of the particle trajectories are quickly localized, while others are diffusing very fast. The slow ones start near to and become trapped in a low potential valley, while the fast particles start from a relatively high value of $U(x)$ and move downhill to a much lower value of $U(x)$, thus experiencing a local energy bias. We note that this phenomenon is analogous to the Golosov localization in standard Sinai diffusion [1,52], when particles starting at the same (thermal) initial position are not significantly separated in the course of time. In the case of exponentially decaying correlations, one may observe two such very close trajectories in Fig. 6(a). Thus, particles diffuse similarly and are correlated. This feature can be very important for the diffusion of proteins on DNA, which may be locally biased, even if the bias is absent on average. This behavior is very different from the scatter of single trajectory averages in the case of annealed continuous-time random-walk subdiffusion with divergent mean resident time. In the latter case, even identical particles starting at the same place will follow very different, diverging trajectories. This feature can therefore be used for a crucial experimental test to distinguish between different types of subdiffusion. Overall, both ensemble and time-averaged mean-squared displacements are by many orders of magnitude faster than in the limit of renormalized normal diffusion whose diffusion coefficient is suppressed by the factor $\exp(-25) \approx 1.39 \times 10^{-11}$, as compared with free normal diffusion in Fig. 6(a) for the same temperature $T = 0.2$. For a typical experimental value $D_0 = 3\ \mu\text{m}^2/\text{s}$ [53] it would become $D_{\rm ren} \approx 4.17 \times 10^{-5}\ \text{nm}^2/\text{s}$, which would mean a practical localization: The particles would diffuse on average over a distance of merely 2 nm within 10^5 s (about 1 day and 4 h).

As can be seen from single trajectory recordings (not shown), particles typically continue their diffusive motion after being localized for a certain time. Indirectly, this feature can also be deduced from some trajectory averages depicted in Fig. 6(a), where the diffusional spread displays a steplike feature. Namely, the diffusional spread continues after temporally reaching a plateau. In data analyses this might mistakingly be attributed to a continuous-time random-walk subdiffusion

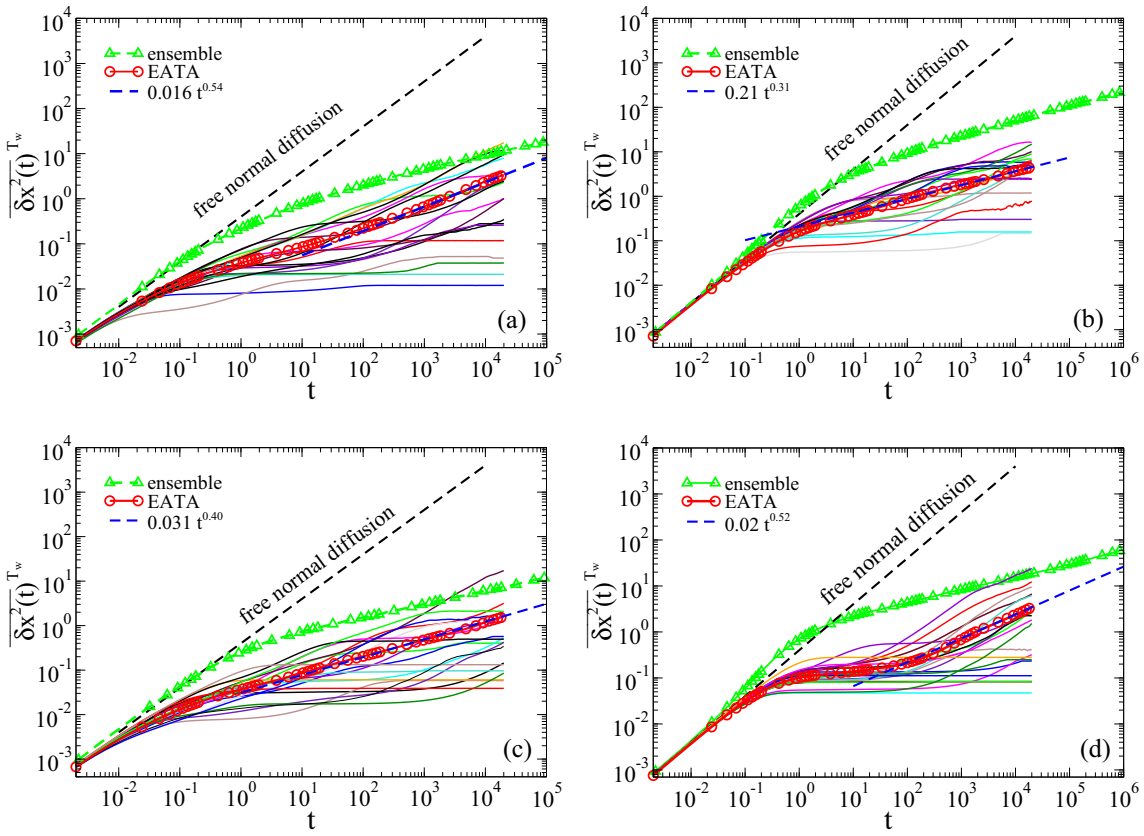

FIG. 6. Single-trajectory, time-averaged mean-squared displacement for $T = 0.2$ and (a) exponential correlations, (b) power-law correlations with $\gamma = 0.8$, (c) linearly decaying correlations, and (d) Gaussian correlation decay. The trajectories time length was $T_w = 2 \times 10^6$. Twenty trajectory averages were made for particles starting from different locations. They are depicted with solid lines. The results of the ensemble-averaged, as well as ensemble-averaged time-averaged (EATA), and free normal mean-squared displacements are also depicted for comparison. The EATA mean-squared displacement is nicely fitted by a power-law dependence, which is also shown in the plot. The asymptotic limit of the disorder-renormalized normal diffusion cannot be plotted for comparison because $D_{\rm ren} = \exp(-25)D_0 \approx 1.39 \times 10^{-11} D_0$, with $D_0 = T = 0.2$. Subdiffusion is by many orders of magnitude faster.

behavior. The ensemble average of the single trajectory time averages is also of interest. This is how experimentalists often proceed to smooth out single trajectory averages [30]. Such an ensemble-averaged time average (EATA) is also shown in Fig. 6. It is nicely fitted by a power-law time dependence. Hence, on the level of this ensemble-averaged time-averaged mean-squared displacement the power-law subdiffusive regime is established earlier.

Also in the case of power-law correlations, single-trajectory averages are broadly scattered, see Fig. 6(b). In this panel, the ensemble-averaged diffusion can be even faster initially than free normal diffusion due to the presence of a local bias. The single trajectory time-averaged mean-squared displacement, however, does not show such a striking feature, see Fig. 6(b). The reasoning for this feature is that the local bias is averaged out in the single trajectory time averaging for a sufficiently large measurement time T_w. Single trajectory averages spread out slower than the ensemble-averaged result and, nevertheless, their broadening is many orders of magnitude faster than the result of the renormalized normal diffusion. This is why even for $\sigma \sim 4$–5, relevant for some important biophysical situations [6,7], regulatory proteins can diffuse on DNA tracks despite the fact that the classical de Gennes–Bässler–Zwanzig result would predict that they should be practically localized (on biophysically relevant time scales) for such a strong disorder. Naturally, single trajectory averages exhibit a large scatter due to a transient lack of ergodicity. It is important to mention that a strong single trajectory scatter was indeed observed experimentally [35]. Note also that such a local bias can be functionally very important, directing the protein toward a specific binding site on DNA. The ensemble-averaged time-averaged mean-squared displacement in this case also shows a power-law scaling in time, see Fig. 6(b). Judging from the power-law exponent $\alpha_{\rm EATA} = 0.31$, it appears to be slower than in the case of exponential correlations, where $\alpha_{\rm EATA} = 0.54$, compare with Fig. 6(a). However, the prefactor in this case is, in fact, much larger, which makes it faster rather than slower.

The scatter of the single-trajectory time-averaged mean-squared displacements is also quite pronounced in the case of linearly decaying correlations, see Fig. 6(c). Such scatter presents a common pattern similarly to other anomalous diffusion processes with nonstationary increments [30,54], in particular, when the systems are aged [51]. Also for Gaussian decay of correlations, the corresponding single trajectory averages are strongly scattered, and their ensemble average

yields a power-law dependence for sufficiently large times, Fig. 6(d).

C. Distribution of first-passage times in a spatial domain

Furthermore, the distribution of first-passage times can be of great interest in applications. All moments of the corresponding residence time distribution in any finite spatial domain are finite. Moreover, the average residence time is much (for a strong disorder $k_BT \ll \sigma$, orders of magnitude) smaller than the one expected from the normal diffusion characterized the renormalized result $D_{\rm ren}$ [23]. In the present case, weak ergodicity breaking does not rely on infinite mean residence times, which makes it especially interesting in biological applications. Residence time distributions of escape times for particles initially located in the center of a symmetric interval $\pm\lambda$ in space for $k_BT \leqslant 0.5\sigma$ for all four types of correlations are nicely described by a generalized log-normal distribution reading

$$\psi(t) = \frac{C}{t}[e^{-|\ln(t/t_m)/\kappa_1|^{b_1}}\theta(t_m - t) + e^{-|\ln(t/t_m)/\kappa_2|^{b_2}}\theta(t - t_m)], \tag{14}$$

where $C = b_1b_2/[b_2\kappa_1\Gamma(1/b_1) + b_1\kappa_2\Gamma(1/b_2)]$ is a renormalization constant, $b_{1,2} > 1$, and $\kappa_{1,2} > 0$. $\Gamma(x)$ denotes the complete Γ function. For any $b_{1,2} > 1$, this distribution (14) has finite moments $\langle t^n\rangle$ of all orders n. For $b_1 = b_2 = 2$ and $\kappa_1 = \kappa_2$, this is the well-known log-normal distribution. However, in our case b_1, b_2, κ_1, and κ_2 are different fitting parameters. Namely, for the exponential correlations $b_1 \approx 2.6$–2.7, and it is weakly temperature dependent. However, b_2 does depend visibly on temperature. For $T = 0.5$, $b_2 = 2$, and it becomes smaller with decreasing temperature while t_m becomes longer. For instance, for $T = 0.2$, $b_2 \approx 1.54$, see Fig. 7(a), where the distribution of times is plotted for the log-transformed variable $\ln t$, attaining a maximum at $\ln t_m$.

For power-law decaying correlations, the escape times in Fig. 7(b) are essentially shorter than in the case of exponential correlations, Fig. 7(a). In particular, the scaling exponent b_2 is larger and the half width κ_2 is smaller. Conversely, the power exponent b_1 is pretty robust, $b_1 \sim 2.6$ (also for other models of disorder, see below).

For linear correlations in Fig. 7(c) one gets $b_1 \sim 2.6$–2.7 nearly independent of temperature, while b_2 also strongly depends on temperature, decreasing with decreasing temperature. All temporal moments of the resident times remain, however, finite with decreasing temperature. Finally, the distribution of the escape times obeys the same common pattern also for Gaussian correlations, as seen in Fig. 7(d).

IV. DISCUSSION

Diffusion in systems characterized by Gaussian fluctuations of the potential with spatially decaying correlations is typically thought of as normally diffusive on experimentally relevant time scales, following the renormalization idea for these systems developed by de Gennes, Bässler, and Zwanzig. This is indeed so for a weak energetic disorder, $\sigma < k_BT$. However, this simple physical picture breaks down in the case of strong disorder featuring many physical systems, including the diffusion of signaling proteins on DNA tracks or colloidal particles in random laser-created potentials. Following recent discoveries of extended anomalous diffusion in such systems, we here provided a clear physical picture for the origin of subdiffusion in stationary Gaussian random potentials with decaying spatial correlations. While the anomalous diffusion is, of course, transient, the scaling theory developed and confirmed herein demonstrates that this transient may easily reach macroscopic time scales for a physically relevant strength of the potential fluctuations.

The primary reason for the origin of this subdiffusion is that the maximal amplitude of the potential fluctuations grows logarithmically with the distance, in accordance with the asymptotic theoretical result (1) and the simulations data depicted in Fig. 1. This behavior is universal, and it has a predictive power. In particular, it allows one to predict for which model of the potential correlations decay the anomalous diffusion will be faster in absolute terms—and this prediction completely agrees with numerics. The strongest trapping effects leading to anomalous diffusion occur in the case of singular models of disorder, such as exponential or linear decays of the correlations, for which the stationary energy autocorrelation function is not differentiable at the origin. This leads to unbounded static force root-mean-squared fluctuations $\langle f^2\rangle^{1/2} \to \infty$ in the strict $\Delta x \to 0$ limit of the coarse graining. Strictly speaking, such models are not amenable to any Langevin simulations unless the random potential is considered on a lattice with a spatial grid Δx, as incorporated in our simulations, with discrete potential points connected by parabolic splines (locally piecewise linear forces). A maximal time step of the Langevin simulations must be chosen accordingly, depending on Δx and the averaged local force root-mean-square $\langle f^2\rangle^{1/2}$. Singular disorder models are regularized accordingly. However, they display the largest potential fluctuations in Fig. 1.

Spatially increasing potential fluctuations may appear strange and contradictory due to the fact that the random potential is stationary and possesses the well-defined root-mean-squared magnitude σ. This property of continuous albeit logarithmic increase with distance is, however, the very cornerstone of the theory of extreme events [40,48]: An extreme event will always occur if only one waits sufficiently long and even if the probability density of such events is strongly localized such as in the case of the considered Gaussian distribution. In our case, the extreme events occur in space rather than time but have the same origin. The law (1) of potential fluctuations with a $(\log x)^\delta$ scaling ($\delta = 1/2$) is valid asymptotically. This argumentation with $x_0 = \Delta x$ in Eq. (1) also holds for disorder, which is uncorrelated on lattice sites, with potential fluctuations even larger than in Fig. 1. Due to the continuity of the potential, the corresponding energetic disorder is actually correlated. However, it is nonstationary, which presents a special case to be studied in detail elsewhere. The longer the spatial correlations of the potential fluctuations reach, the later this asymptotic is achieved. The convergence to an extreme value distribution is known to be very slow also for independent Gaussian variables [48]. Numerically, we also observed different scaling exponents such as $\delta = 1$ transiently and $\delta > 1$ initially.

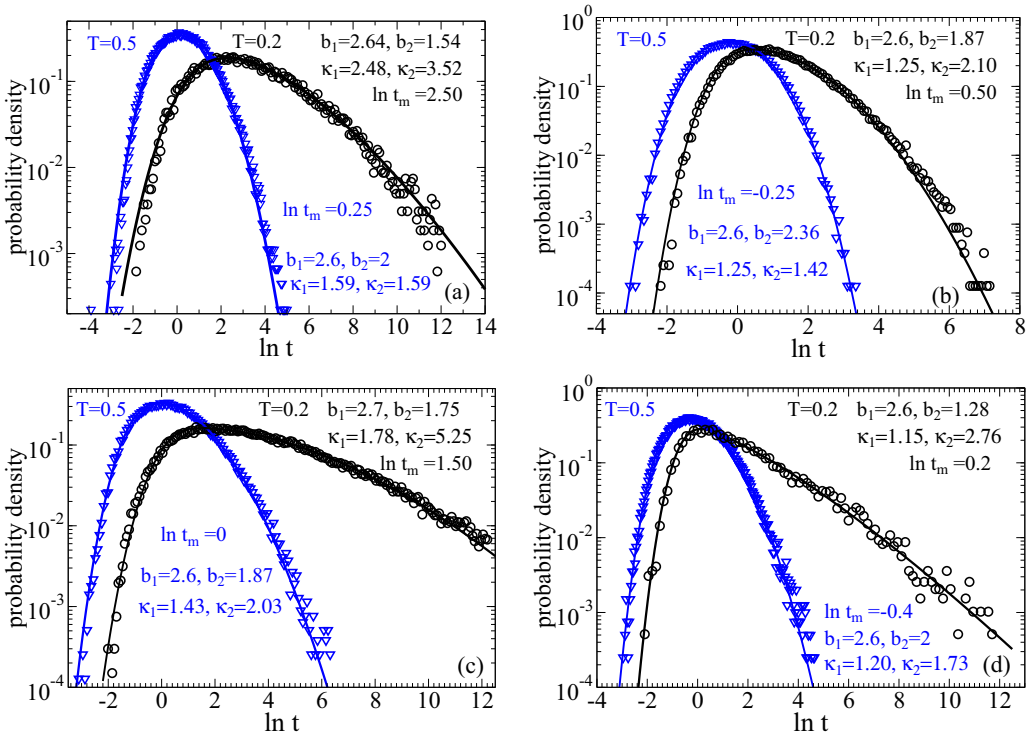

FIG. 7. Probability density function of log-transformed first escape times from the interval $[-\lambda,\lambda]$ for two temperatures $T = 0.5$ (in blue) and $T = 0.2$ (in black). The cases in the different panels are (a) exponential correlations, (b) power-law correlations with $\gamma = 0.8$, (c) linearly decaying correlations, and (d) Gaussian correlation decay. The symbols represent simulations data, the lines correspond to a fit with the probability density (14). Parameters are shown in the panels. With decreasing temperature the distributions become broader and the parameter b_2 smaller.

Based on these observations we put forward a very simple scaling theory of anomalous diffusion in the potential landscape $U(x)$, which in essence is very similar to the scaling theory of Sinai diffusion developed in Ref. [1]. It leads to our major result given in Eq. (3) and explains why for sufficiently low temperatures we indeed observe a generalized Sinai diffusion with a power-law exponent, which is generally different from $a = 4$ and can be even smaller as shown in Figs. 2(b), 2(c) and 2(d): The diffusion is formally even slower than for the case of Sinai diffusion in random force fields. Our analytical results were shown to be valid over 5 to 7 decades in time, at least, which is a remarkable success of the relatively simple scaling approach. The nominally ultraslow diffusion is in fact many orders of magnitude faster than the asymptotical limit of the disorder-renormalized normal diffusion, which for the physically relevant parameters considered here simply cannot be attained either physically or numerically for such a strong disorder. Hence, it becomes completely irrelevant in such settings. This provides a striking example of how the formally valid mathematical result of asymptotic, disorder-renormalized normal diffusion in the de Gennes–Bässler–Zwanzig theory may produce physically inappropriate descriptions on meso- and macroscales.

This result also leads to a number of further predictions, which are confirmed in numerical simulations and agree with previous simulations of the considered stochastic dynamics in random potentials. Namely, this kind of anomalous diffusion is generally characterized by a time-dependent power-law exponent $\alpha(t)$, for which we obtained the theoretical result (6). This result predicts that, after an initial decay ($\delta > 1$), the anomalous diffusion exponent $\alpha(t)$ will reach a minimum for which $\alpha_{\min} = 2k_BT/\sigma_{\text{eff}}$ (for $\delta = 1$) and then gradually grow in logarithmic fashion, $\alpha(t) = 2(k_BT/\sigma_{\text{eff}})^2 \ln(t/t_0)$ ($\delta = 1/2$). These two nontrivial predictions are remarkably well confirmed by extensive numerical simulations. Indeed, $\alpha_{\min} = 2k_BT/\sigma_{\text{eff}}$ with $\sigma_{\text{eff}} \sim 1.24$–$1.52$, within a broad range of temperatures, as demonstrated in Fig. 3. Moreover, at sufficiently large temperatures, $\alpha(t)$ grows logarithmically, see Fig. 3. It is indeed remarkable how a simple scaling theory can be predictive to such a degree. Of course, the scaling results cannot be fully accurate on a quantitative level and claim full consistency over the entire range of parameters and times studied herein. In particular, the values of σ_{eff} and t_0 used to fit the numerical data, for instance, in Figs. 2 and 3 are in fact different. This is due to the fact that the approximation of Eq. (3) by Eqs. (5) and (6) is, indeed, a bit too coarse. Nevertheless, the coherence and validity of our scaling theoretical predictions are compelling.

We note that in the biologically relevant and important case of power-law decaying correlations the scaling $\delta = 1$ applies to a much larger range of times and temperatures, as shown in Figs. 2(c) and 3(b). In this case, power-law subdiffusion of the form $\langle \delta x^2(t) \rangle \propto t^\alpha$ with $\alpha \approx 1.41\, k_BT/\sigma$ in fact presents a good approximation over a broad range of times and temperatures. This behavior may easily be confused with the law $\alpha \approx k_BT/\sigma$ produced by the mean-field continuous-time

random-walk with exponential energy disorder [19,20,25]. In striking contrast to the latter model, however, the residence times in a finite spatial domain are not power-law distributed but follow the generalized log-normal distribution (14) shown in Fig. 7 for all the studied models of the correlation decay. All moments of this distribution are finite, which is a very attractive physical feature. This subdiffusion is clearly nonergodic, as demonstrated in Fig. 6, where the maximal time is merely 1% of the time window T_w used to accumulate the single-trajectory averages. Hence, a large scatter is a truly nonergodic effect, even if it is a transient one and must vanish in the mathematical limit $T_w \to \infty$ [23]. It is, however, not necessarily attainable experimentally.

The origin of this lack of ergodicity was already explained in Ref. [23]: It is due to the absence of self-averaging of the statistical weight function $w(x) = \exp[\pm\beta U(x)]$ on the spatial scale $L_{\rm erg}$, implicitly defined in relation (8), depending on the disorder autocorrelation function $g(x)$. Solving this equation analytically in the case of linearly decaying correlations yields the exact result (9) and a very handy and highly accurate approximate result in Eq. (10). In this case of linear decay, $L_{\rm erg}$ turns out to be the shortest one within all models of $g(x)$ considered in this paper, see Table I. This result implies that $L_{\rm erg}$ in units of the correlation scale λ is only by a factor $(1/2)(\sigma/k_BT)^2$ smaller than the factor $\exp[\sigma^2/(k_BT)^2]$ suppressing the asymptotically normal diffusion coefficient in the renormalization sense. This, in turn, means that such mesoscopic subdiffusion can readily reach macroscopic scales even for a moderate disorder strength $\sigma \sim 4$–$5\, k_BT$ featuring many physical and biological systems already at room temperatures.

Different from the annealed continuous-time random-walk subdiffusion, the single trajectory time averages for the mean-squared displacement in the present case of quenched potential fluctuations are characterized by different power-law exponents $\alpha \neq 1$ [23] and not just a linear scaling with the lag time (erroneously suggesting normal diffusion) but with a significantly scattered diffusion coefficient [32,33]. Importantly, especially with respect to biological applications is that the subdiffusion considered here is in fact orders of magnitude faster than the normal diffusion predicted by the classical renormalization result with effective diffusivity $D_{\rm ren}$. For example, for the diffusion of regulatory proteins on DNA tracks, $\sigma \approx 4.3\, k_BT_{\rm room}$, which can be deduced from the results presented in Ref. [7]. Hence, $D_{\rm ren} = 9.33 \times 10^{-9} D_0$, and for a typical experimental value $D_0 = 3\ \mu{\rm m}^2/{\rm s}$ [53] it would become $D_{\rm ren} \approx 2.8 \times 10^{-2}{\rm nm}^2/{\rm s}$. This would mean that within some hundreds of seconds the diffusional spread would be merely several nanometers. However, this renormalization result underestimates massively, on the relevant time scales of this phenomenon, the actual protein mobility. Our results demonstrate that the actually occurring subdiffusion is orders of magnitude faster than one suggested by this normal diffusion result of the renormalization approach. Hence, correlations-induced persistent subdiffusion makes diffusional search feasible in such a situation despite a strong binding-energy disorder.

An important role in applications may also be played by the presence of a local bias, which is especially clearly expressed in the case of power-law correlations. This is the analogous reason for the Golosov phenomenon in the case of random potential exhibiting Brownian motion in space [1]. Then the particles which were initially localized nearby diffuse similarly, in a correlated fashion. The distance between them does not grow dramatically in time, being bounded. One can find similar single trajectory averages also in our numerical results. Conversely, different particles starting in locally different environments can move into opposite directions, and this can give rise to an enhanced diffusivity in the ensemble sense. In fact, for this reason an initial regime of superdiffusion can be realized in Fig. 6(b) and 6(d) on the ensemble level in the case of power-law correlations and Gaussian correlations, respectively, for which it can extend over several scaling lengths λ, see also Fig. 3(b) and 3(d) for small times. In the case of single trajectory time averages, the local bias averages out. Therefore, such a superdiffusive regime is absent. Diffusion on the level of single trajectories is typically slower than the one on the ensemble level, see, for instance, Fig. 6. The difference between the ensemble average and the ensemble-averaged time average of the mean-squared displacement becomes smaller with increasing time. The latter ensemble time averages display a power-law dependence on time for sufficiently large times even in the Sinai-like regime on the ensemble level, which can be an important observation with respect to possible experimental manifestations.

V. CONCLUSION

To conclude, we elucidated the physical mechanism leading to subdiffusion in stationary correlated potentials with spatially decorrelating Gaussian disorder, and we showed that a generalized Sinai diffusion typically emerges at sufficiently low temperatures and/or strong disorder for various models of decaying correlations. Our scaling theory also explains how a standard power-law subdiffusion emerges with increasing temperature and in the course of time. Such subdiffusion is weakly nonergodic, displays a local bias, and proceeds much faster than de Gennes–Bässler–Zwanzig limit of normal diffusion, which for sufficiently low temperatures and/or finite size of the system simply cannot be attained physically on typical mesoscales. We believe that our results provide a new vista on the old problem of potential disorder and that they will be very useful in the context of nonergodic diffusion processes, especially in relation to various biologically relevant problems on the cellular level. Likely they are also important for diffusion of colloidal particles in laser created random potentials, a conjecture calling for further experimental studies of such systems.

ACKNOWLEDGMENT

Funding of this research by the Deutsche Forschungsgemeinschaft (German Research Foundation), Grant No. GO 2052/3-1, is gratefully acknowledged.

[1] J.-P. Bouchaud and A. Georges, Phys. Rep. **195**, 127 (1990).

[2] J. Bouchaud, A. Comtet, A. Georges, and P. L. Doussal, Ann. Phys. (NY) **201**, 285 (1990).

[3] H. Bässler, Phys. Status Solidi B **175**, 15 (1993).

[4] D. H. Dunlap, P. E. Parris, and V. M. Kenkre, Phys. Rev. Lett. **77**, 542 (1996).

[5] H. Bässler, Phys. Rev. Lett. **58**, 767 (1987).

[6] U. Gerland, J. D. Moroz, and T. Hwa, Proc. Natl. Acad. Sci. USA **99**, 12015 (2002).

[7] M. Lässig, BMC Bioinform. **8**, S7 (2007).

[8] M. Slutsky, M. Kardar, and L. A. Mirny, Phys. Rev. E **69**, 061903 (2004).

[9] F. Evers, R. D. L. Hanes, C. Zunke, R. F. Capellmann, J. Bewerunge, C. Dalle-Ferrier, M. C. Jenkins, I. Ladadwa, A. Heuer, R. Castaneda-Priego, and S. U. Egelhaaf, Eur. Phys. J. Spec. Top. **222**, 2995 (2013).

[10] R. D. L. Hanes and S. U. Egelhaaf, J. Phys.: Condens. Matter **24**, 464116 (2012).

[11] R. D. L. Hanes, M. Schmiedeberg, and S. U. Egelhaaf, Phys. Rev. E **88**, 062133 (2013).

[12] J. Bewerunge and S. U. Egelhaaf, Phys. Rev. A **93**, 013806 (2016).

[13] P. Hänggi, P. Talkner, and M. Borkovec, Rev. Mod. Phys. **62**, 251 (1990).

[14] P. G. D. Gennes, J. Stat. Phys. **12**, 463 (1975).

[15] R. Zwanzig, Proc. Natl. Acad. Sci. USA **85**, 2029 (1988).

[16] T. Hecksher, A. I. Nielsen, N. B. Olsen, and J. C. Dyre, Nat. Phys. **4**, 737 (2008).

[17] A. H. Romero and J. M. Sancho, Phys. Rev. E **58**, 2833 (1998).

[18] Indeed, quenched mean-field RTD can be represented as a sum (integral) over exponential contributions, $\psi(t) = \int_0^\infty \frac{1}{\tau} e^{-t/\tau} \rho(\tau) d\tau$, with relaxation time constants $\tau(U)$, which depend on the activation barrier U in an Arrhenius manner, $\tau(U) = \tau_0 e^{\beta U}$, with τ_0 being a prefactor constant. The distribution $\rho(\tau)$ of τ is expressed via distribution of the barrier heights $P(U)$ as $\rho(\tau) = P(U)|dU/d\tau|$. For a Gaussian $P(U) = \frac{1}{\sqrt{2\pi\sigma^2}} e^{-U^2/(2\sigma^2)}$, $\rho(\tau) = \frac{1}{\sqrt{2\pi}\sigma\beta\tau} e^{-\frac{\ln^2(\tau/\tau_0)}{2(\beta\sigma)^2}}$ is log-normal, and all the moments $\langle t^n \rangle = \int_0^\infty t^n \psi(t) dt = n! \int_0^\infty \tau^n \rho(\tau) d\tau = n! \tau_0^n e^{(n\beta\sigma)^2/2}$, $n = 1,2,...,$ are finite.

[19] B. D. Hughes, *Random Walks and Random Environments* (Clarendon Press, Oxford, 1995).

[20] R. Metzler and J. Klafter, Phys. Rep. **339**, 1 (2000).

[21] M. Schubert, E. Preis, J. C. Blakesley, P. Pingel, U. Scherf, and D. Neher, Phys. Rev. B **87**, 024203 (2013).

[22] H. Scher and E. W. Montroll, Phys. Rev. B **12**, 2455 (1975).

[23] I. Goychuk and V. O. Kharchenko, Phys. Rev. Lett. **113**, 100601 (2014).

[24] C.-K. Peng, S. V. Buldyrev, A. L. Goldberger, S. Havlin, F. Sciortino, M. Simons, and H. E. Stanley, Nature (London) **356**, 168 (1992).

[25] D. ben Avraham and S. Havlin, *Diffusion and Reactions in Fractals and Disordered Systems* (Cambridge University Press, Cambridge, 2000).

[26] M. Khoury, A. M. Lacasta, J. M. Sancho, and K. Lindenberg, Phys. Rev. Lett. **106**, 090602 (2011).

[27] M. S. Simon, J. M. Sancho, and K. Lindenberg, Phys. Rev. E **88**, 062105 (2013).

[28] J. P. Bouchaud, J. Phys. I France **2**, 1705 (1992).

[29] G. Bel and E. Barkai, Phys. Rev. Lett. **94**, 240602 (2005).

[30] R. Metzler, J.-H. Jeon, A. G. Cherstvy, and E. Barkai, Phys. Chem. Chem. Phys. **16**, 24128 (2014).

[31] S. Burov and E. Barkai, Phys. Rev. Lett. **98**, 250601 (2007).

[32] A. Lubelski, I. M. Sokolov, and J. Klafter, Phys. Rev. Lett. **100**, 250602 (2008).

[33] Y. He, S. Burov, R. Metzler, and E. Barkai, Phys. Rev. Lett. **101**, 058101 (2008).

[34] I. Sokolov, E. Heinsalu, P. Hänggi, and I. Goychuk, Europhys. Lett. **86**, 30009 (2009).

[35] Y. M. Wang, R. H. Austin, and E. C. Cox, Phys. Rev. Lett. **97**, 048302 (2006).

[36] Ya. G. Sinai, Theor. Prob. Appl. **27**, 256 (1983).

[37] P. Le Doussal, C. Monthus, and D. S. Fisher, Phys. Rev. E **59**, 4795 (1999).

[38] A. Godec, A. V. Chechkin, E. Barkai, H. Kantz, and R. Metzler, J. Phys. A **47**, 492002 (2014).

[39] G. Oshanin, A. Rosso, and G. Schehr, Phys. Rev. Lett. **110**, 100602 (2013).

[40] E. Castillo, A. S. Hadi, N. Balakrishnan, and J. M. Sarabia, *Extreme Value and Related Models with Applications in Engineering and Science* (John Wiley & Sons, Hoboken, NJ, 2004).

[41] J. Pickands, Trans. Amer. Math. Soc. **145**, 51 (1969).

[42] Y. C. Zhang, Phys. Rev. Lett. **56**, 2113 (1986).

[43] A. Papoulis, *Probability, Random Variables, and Stochastic Processes*, 3rd ed. (McGraw–Hill, New York, 1991).

[44] O. Bénichou, Y. Kafri, M. Sheinman, and R. Voituriez, Phys. Rev. Lett. **103**, 138102 (2009).

[45] M. Bauer, E. S. Rasmussen, M. A. Lomholt, and R. Metzler, Sci. Rep. **5**, 10072 (2015).

[46] M. S. Simon, J. M. Sancho, and A. M. Lacasta, Fluct. Noise Lett. **11**, 1250026 (2012).

[47] A. J. Stewart, S. Hannenhalli, and J. B. Plotkin, Genetics **192**, 973 (2012).

[48] R. A. Fisher and L. H. C. Tippett, Proc. Cambridge Phil. Soc. **24**, 180 (1928).

[49] A. M. Yaglom, *An Introduction to the Theory of Stationary Random Functions* (Dover, New York, 1972).

[50] S. Lifson and J. L. Jackson, J. Chem. Phys. **36**, 2410 (1962).

[51] J. H. P. Schulz, E. Barkai, and R. Metzler, Phys. Rev. X **4**, 011028 (2014).

[52] A. O. Golosov, Commun. Math. Phys. **92**, 491 (1984).

[53] J. Elf, G.-W. Li, and X. S. Xie, Science **316**, 1191 (2007).

[54] J.-H. Jeon, M. Javanainen, H. Martinez-Seara, R. Metzler, and I. Vattulainen, Phys. Rev. X **6**, 021006 (2016).